

# Insights into friction dependence of carbon nanoparticles as oil-based lubricant additive at amorphous carbon interface

Xiaowei Li <sup>a, b, \*</sup>, Xiaowei Xu <sup>b</sup>, Yong Zhou <sup>b</sup>, Kwang-Ryeol Lee <sup>a, \*\*,</sup>, Aiyang Wang <sup>b, \*\*\*</sup>

<sup>a</sup> Computational Science Center, Korea Institute of Science and Technology, Seoul, 136-791, Republic of Korea

<sup>b</sup> Key Laboratory of Marine Materials and Related Technologies, Zhejiang Key Laboratory of Marine Materials and Protective Technologies, Ningbo Institute of Materials Technology and Engineering, Chinese Academy of Sciences, Ningbo, 315201, PR China

## ARTICLE INFO

### Article history:

Received 27 February 2019

Received in revised form

19 May 2019

Accepted 20 May 2019

Available online 22 May 2019

## ABSTRACT

Solid-liquid lubricating system, composed of amorphous carbon (a-C) and fluid lubricant, arouses enormous interest due to its excellent tribological performance. However, the friction response of a-C induced by carbon nanoparticles including graphene (G), fullerene (C60), and carbon nanotube (CNT) as oil-based additives and the underlying friction mechanism in synergism with base oil are unclear. Herein, using reactive molecular dynamics simulation, we comparatively investigated the friction dependence of G, C60, and CNT additives at the a-C interface. Compared with pure base oil, G results in the friction coefficient reduced by 90%, which exhibits the best anti-friction ability than C60 and CNT. The interfacial structure transformation, the interaction between the a-C, base oil, and additives, and the mobility of base oil indicate that being different with C60 or CNT which cross-links both the mating a-C surfaces, the G only anchors to one a-C surface to form a block physical protective film, which significantly smooths a-C surface, weakens the intermolecular interaction of a-C with base oil, and thus promotes the mobility of oil molecules, presenting a synergistic effect on the friction performance. These address the fundamental understanding on carbon additive-induced friction mechanism, and guide the design of a-C/lubricant composite system for tribological applications.

© 2019 Elsevier Ltd. All rights reserved.

## 1. Introduction

Friction exists in almost all mechanical systems with moving components, causing large amounts of energy dissipation (about 20%), materials losses, and CO<sub>2</sub> emissions every year, which has become a globally urgent task to develop the advanced lubricating system for aerospace, automotive, military, and various industrial applications [1,2]. In order to minimize the risk of friction-induced mechanical failure and improve the machine efficiency, solid-liquid lubricating system, which makes full use of the advantages of solid lubricating film and the unique property of fluid lubricant, has been widely regarded as a more effective strategy than single component [3–5]. Especially due to the excellent mechanical and low-friction

properties, amorphous carbon (a-C) film is a strong candidate as solid lubricating part to cooperate with fluid lubricant [6–8], improving the durability and reliability of mechanical components in synergism.

It is well known that besides the base oil, fluid lubricant normally contains a variety of nanomaterials as additives [9–14], which are dispersed in the base oil to not only stabilize the fluid lubricant, but also enhance the comprehensive performance of solid-liquid lubricating system, which is of paramount importance for engineering and technical applications. Among of them, carbon-based nanoparticles, especially graphene (G) [15–19], fullerene [20–22], and carbon nanotube (CNT) [23–25], are qualified to be effective solid anti-friction additives owing to their unique structure and exceptional properties. For the G with 2D structure, notable mechanical and load-bearing capacities, and atomically smooth surface, Eswarajah et al. [15] studied the tribological property of G-based engine oil and found that the friction coefficient, anti-wear, and extreme pressure properties were reduced by 80%, 33%, and 40%, respectively, compared with the base oil, attributing to the nanobearing mechanism and high mechanical strength of G in engine oil. Zin et al. [16] revealed that graphene-

\* Corresponding author. Computational Science Center, Korea Institute of Science and Technology, Seoul, 136-791, Republic of Korea.

\*\* Corresponding author.

\*\*\* Corresponding author.

E-mail addresses: [lixw0826@gmail.com](mailto:lixw0826@gmail.com) (X. Li), [krlee@kist.re.kr](mailto:krlee@kist.re.kr) (K.-R. Lee), [aywang@nimte.ac.cn](mailto:aywang@nimte.ac.cn) (A. Wang).

based nano-additive resulted in a maximum decrease of 18% in friction coefficient and over 70% in worn volume estimated under boundary lubrication condition because of the reduced contact area. However, Luo [18] and Mao [19] reported the formation of a continuous “protective film” or “tribofilm” caused by G, which prevented the rubbing surfaces from direct contact and thus led to the exceptional lubrication behavior. As the fullerene and its derivatives were considered as additives, Yao et al. [20] showed that due to the unique spherical shape and highly symmetric structure of fullerene, it not only served as spacer to inhibit the rough contact between the two mating surfaces, but also provided easily slider or roll of mating surface, named as “rolling effect”, accounting for the low-friction behavior, which was also proved by Matsumot [21] and Zhang [22]. For CNT with high tensile and flexural strength, Gong et al. [23] found that a protective film was generated on the wear surface, contributing to the low friction and high wear resistance of CNT derivatives, which agreed with Meng [24] and Salah's [25] reports.

The above-mentioned results demonstrated the friction mechanisms (nanobearing, interlamination sliding, reduced contact area, transfer or protective film, rolling effect) of carbon nanoparticles as additives in base oil [15–25]. However, on the one hand, due to the limited characterization of interfacial structure evolution and the difference in both the types of nanoparticles and derivatives and the volatile working environments, it remains a big challenge to completely clarify the friction mechanism of carbon nanoparticles in experiment until now. The in-depth understanding from the atomic scale is required to disclose the exact friction mechanism induced by G, CNT, and fullerene. On the other hand, to the best of our knowledge, most of previous studies were designed for metal-to-metal contact surface [15–25], the friction behavior of G, fullerene, and CNT as oil-based additives on the a-C surface, the interaction between the a-C, base oil, and additives, and the underlying mechanism in synergism are still unclear, which is requisite for the development and application of advanced a-C/lubricant composite lubricating system.

In this work, we conducted reactive molecular dynamics (RMD) simulation to study the friction behavior of a-C composited with fluid lubricant. The linear alpha olefin,  $C_8H_{16}$ , was selected as base oil [26], while G, C60 as fullerene, and CNT were regarded as lubricant additives to comparatively evaluate the dependence of friction response on the additive variety. Most importantly, the evolution of interfacial structure and the interaction between the additives,  $C_8H_{16}$ , and a-C, and the mobility of fluid lubricant were investigated systematically to shed light on the synergistic friction mechanism. Results revealed the friction behavior of a-C strongly depended on the lubricant additive, and the G structure was suggested to cooperate with base oil for high anti-friction performance.

## 2. Computational methods

All simulations were employed by Large-scale atomic/molecular massively parallel simulator (LAMMPS) code [27]. Fig. 1 showed the “Sandwich” model of a-C/lubricant/a-C friction system used in the present work, which was divided into lower a-C substrate, fluid lubricant, and upper a-C counterface. The mating a-C structure with size of  $42.88 \times 40.358 \times 31 \text{ \AA}^3$  and 6877 carbon atoms was deposited by an atom-by-atom method [28], and it had an  $sp^3$  fraction of 24 at.%, an  $sp^2$  fraction of 72 at.%, and a density of  $2.7 \text{ g/cm}^3$ . Fluid lubricant was composed of base oil and additives, in which  $C_8H_{16}$  was considered as a representative lubricating oil and the number of  $C_8H_{16}$  molecules was fixed at 45 [26]. In order to conduct a comparative study on the friction response of a-C induced by different additives, the carbon nanoparticle fragments including G, C60, and CNT were selected as additives, but the number of C atoms

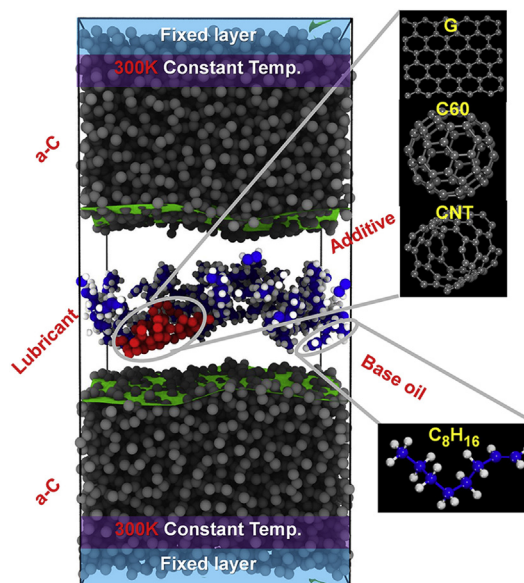


Fig. 1. Simulated model for a-C/lubricant/a-C friction system. (A colour version of this figure can be viewed online.)

for each additive fragment was fixed at 60, and the corresponding additive content was 12.5 wt%. The separation distance between the lubricant and the lower or upper a-C film was  $3 \text{ \AA}$ .

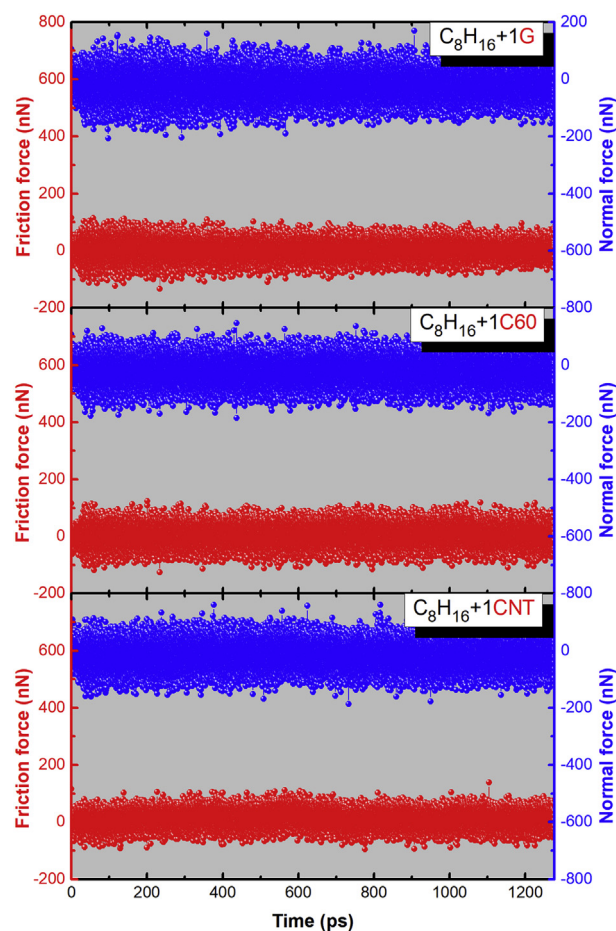
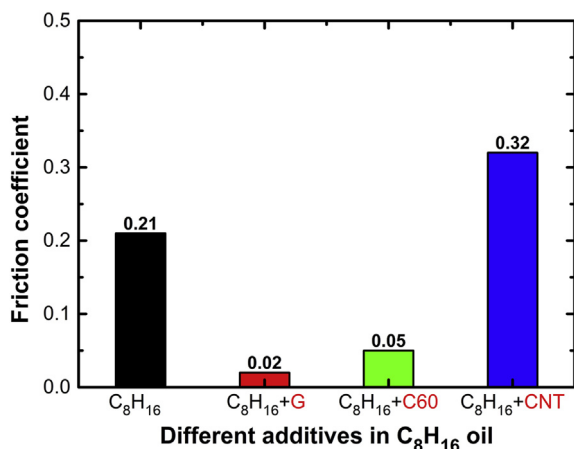


Fig. 2. Friction curves including friction and normal forces with sliding time for each case. (A colour version of this figure can be viewed online.)



**Fig. 3.** Friction coefficient with different additives. (A colour version of this figure can be viewed online.)

Similar to previous study [3,26], a three-layer assumption model was applied to each a-C/lubricant/a-C system, including the fixed layer (blue background in Fig. 1) for simulating the semi-infinite system, the thermostatic layer (purple background in Fig. 1) being maintained at 300 K through the *NVE* ensemble with a Berendsen thermostat [29], and the free layer consisted of the remnant a-C and lubricant ( $C_8H_{16}$  and additive) in Fig. 1 for modeling the friction-induced structure evolution at the interface. Time step was 0.25 fs and periodic boundary condition was imposed along both the *x*- and *y*-directions. ReaxFF potential developed by Tavazza et al. [30] was utilized to accurately describe the C–C, C–H, and H–H interactions in the whole system, whose reliability has been validated by our previous works [3,26,31].

During the friction process, a three-step process was adopted: (i) geometric optimization at 300 K for 2.5 ps; (ii) loading process to achieve the specified value of contact pressure (5 GPa) during 25 ps; (iii) sliding process with a fixed contact pressure and a sliding velocity of 10 m/s along the *x*-direction for 1250 ps. Our [3,26] and previous studies [32–35] have already confirmed that the high contact pressure (5 GPa) was appropriate to examine the friction behavior on an atomic scale. After the friction process, the forces acting on the fixed atoms of bottom a-C layer (blue region at the bottom of Fig. 1) in the *x* and *z* directions were counted as the friction force, *f*, and normal force, *W*, respectively, to calculate the friction coefficient for each case. The detailed process was described in our previous work [3].

### 3. Results and discussion

Fig. 2 shows the friction curves including friction and normal forces with sliding time for each system. It can be seen that compared with the pure a-C/a-C friction system [31], after adding the G, C60, or CNT as oil-based additive into the friction interface, the friction process reaches the stable friction stage quickly without the obvious running-in process, which is close to the case with  $C_8H_{16}$  only [26]. The absence of running-in process is ascribed to the low contact pressure and the chemical bonding of mating a-C surfaces shielded by lubricant [3]. In order to quantify the effect of different additives on the friction property, the values obtained during the last 200 ps of stable friction stage (Fig. 2) are employed to calculate the friction and normal forces for each case, as shown in Fig. S1 of Supplementary Information. First, by comparing with the additive-free case, with the additive ranged from G, C60 to CNT, there is almost no additional rise of flash temperature at the friction interface, which is kept at about 300 K. Interestingly, the normal force with additive variety displays a slight difference, which is

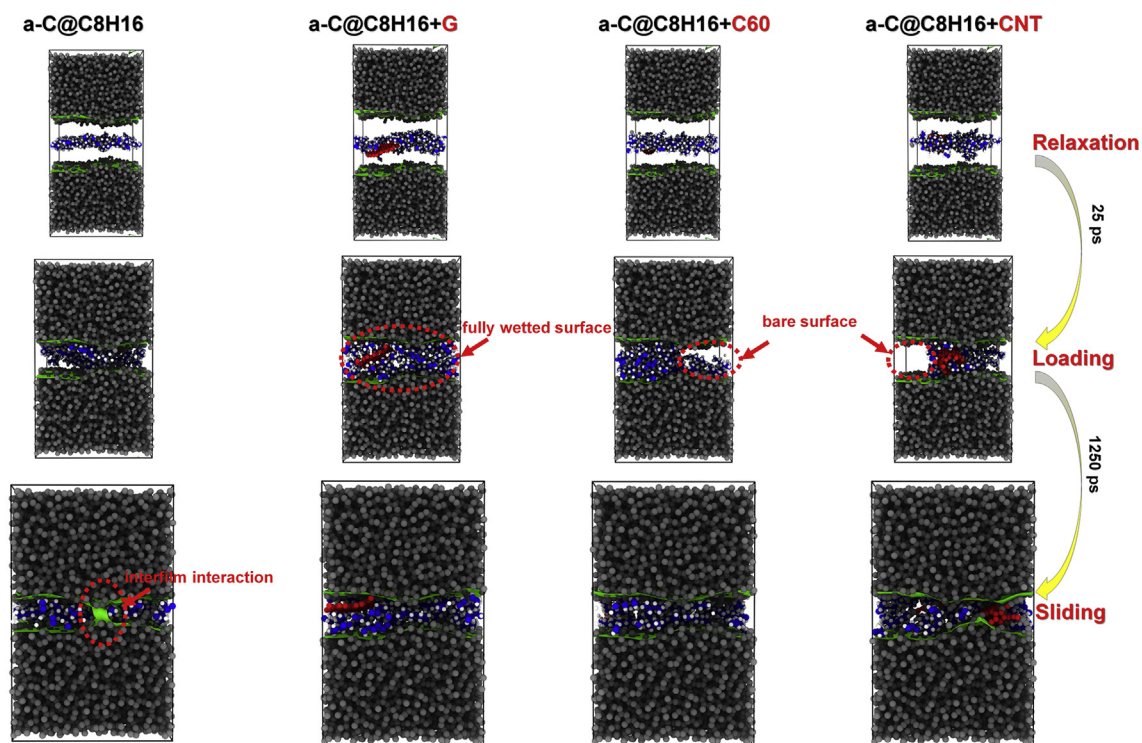


**Fig. 4.** Morphologies of self-mated a-C@ $C_8H_{16}$  systems with different additives (G, C60, and CNT), in which gray, blue, and red colors represent C atoms from a-C, base oil, and additive, respectively, white color represents H atom, and green color is the surface mesh of a-C mating materials. (A colour version of this figure can be viewed online.)

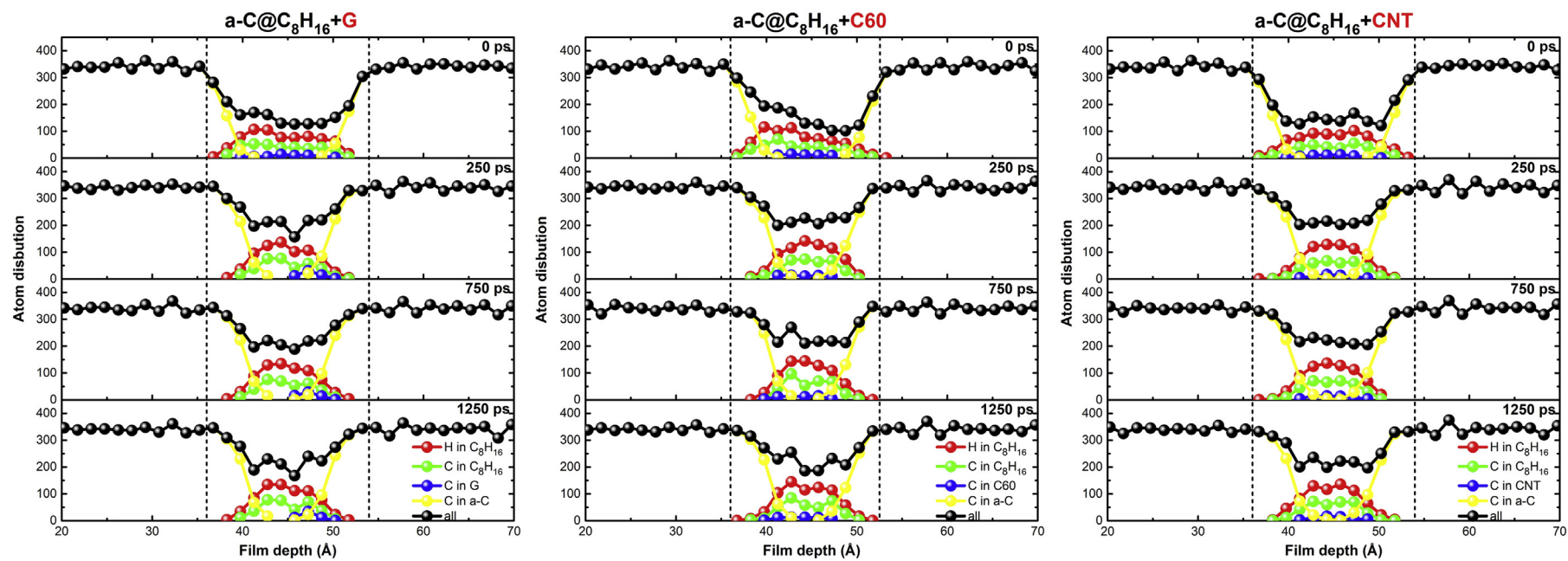


**Fig. 5.** Atomic distributions along the film depth direction for each case, which are contributed by the total, C in a-C, C in additive (G, C60, and CNT), and C and H in  $C_8H_{16}$  base oil, respectively. (A colour version of this figure can be viewed online.)

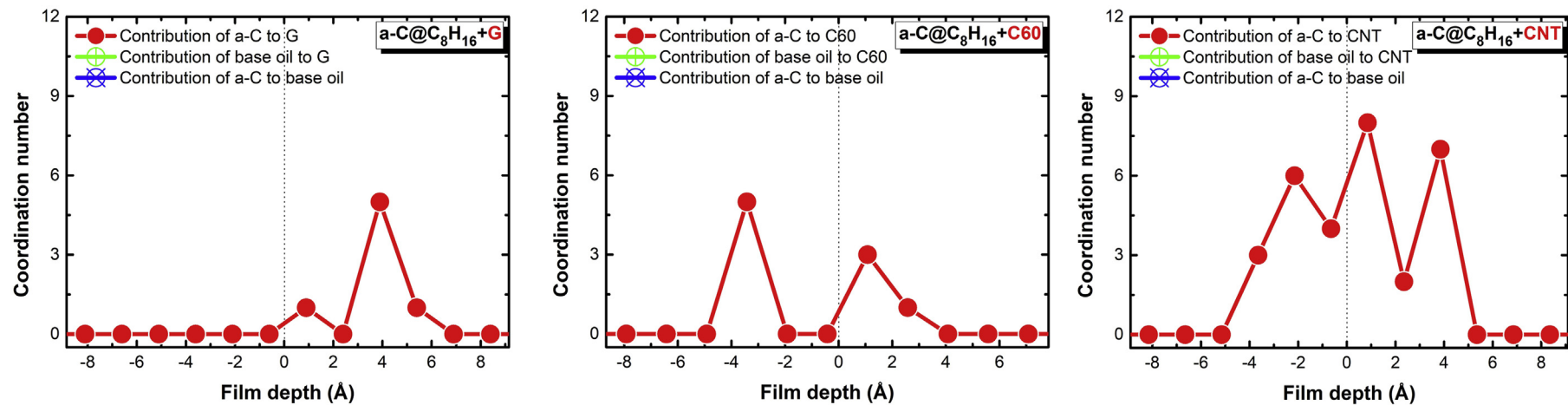


Fig. 6. Coordination number contribution between the base oil, additives, and a-C films at the sliding time of 1000 ps.

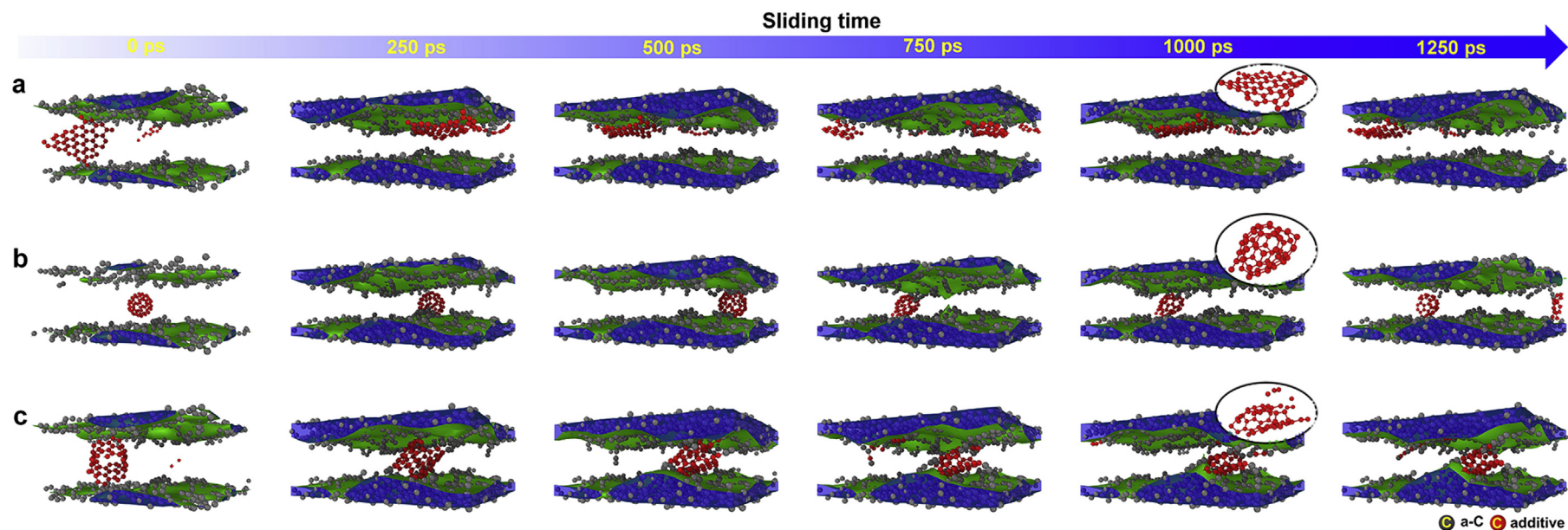


Fig. 7. Transformation of interfacial structure of (a) a-C@C<sub>8</sub>H<sub>16</sub>+G, (b) a-C@C<sub>8</sub>H<sub>16</sub>+C60, and (c) a-C@C<sub>8</sub>H<sub>16</sub>+CNT systems with sliding time, in which the C<sub>8</sub>H<sub>16</sub> base oil is neglected for view. (A colour version of this figure can be viewed online.)

related with the real contact zone at the friction interface, but the friction force obviously increases from 0.56 for G to 1.18 for C60 and 7.05 nN for CNT. In particular, the friction force in G- or C60-contained system is much smaller than that in a-C@C<sub>8</sub>H<sub>16</sub> system (5.23 nN), while it increases significantly when CNT is considered as additive, implying the different and significant evolution of interfacial structure and the potential collapse of additive structure, as will be discussed later.

According to the friction and normal force values, Fig. 3 shows the calculated friction coefficient in each friction system, and the result from a-C/C<sub>8</sub>H<sub>16</sub>/a-C system is also provided for comparison [26]. It reveals that the friction coefficient is strongly dependent on the additive variety in base oil, consistent with the evolution of friction force in Fig. S1 of Supplementary Information. For the a-C friction system with C<sub>8</sub>H<sub>16</sub> as base oil only, the friction coefficient is 0.21, which is higher than that in experiment. This is owing to the used a-C structure without any surface contamination or passivation, inducing the high adhesive strength of mating materials [3,31]. After introducing G or C60 into the base oil, the friction coefficient decreases to 0.02 for G or 0.05 for C60, which is reduced by 90% or 76%, respectively, by comparing with the additive-free case. However, the opposite increase of friction coefficient from 0.21 to 0.32 is observed for a-C@C<sub>8</sub>H<sub>16</sub>+CNT system. This implies that the graphene fragment is the best candidate as oil-based additive than C60 and CNT to cooperate with the base oil and a-C for enhancing the anti-friction performance maximally, which is similar to previous works [4,20,21].

In order to clarify the fundamental effect of different additives on the friction behavior, Fig. 4 first illustrates the morphologies of

self-mated a-C@C<sub>8</sub>H<sub>16</sub> systems with different additives after the friction process, and the morphologies after relaxation and loading processes are also provided for comparison. Note that after the loading process, the fluid lubricant with G as additive can fully wet the a-C surface, while the bare a-C is observed in both the a-C@C<sub>8</sub>H<sub>16</sub>+C60 and a-C@C<sub>8</sub>H<sub>16</sub>+CNT cases, which may induce the direct contact of rough surface and thus lead to the high friction coefficient. After the sliding process of 1250 ps, the morphology of a-C@C<sub>8</sub>H<sub>16</sub> system shows that most of the mating a-C films could be separated by the C<sub>8</sub>H<sub>16</sub> lubricant with slight direct interfilm interaction, suggesting the improvement of friction behavior of a-C/a-C system via the hydrodynamic lubrication of base oil [26]. However, by introducing G, C60, or CNT fragments as additives into the base oil, the inter-interaction between the mating a-C films is completely prevented by the fluid lubricant following the increased separation distance, but there is an obvious difference in the interfacial structure and a-C surface observed for each case, which is also confirmed by the atom distribution along the film depth direction, as shown in Fig. 5.

In addition, Fig. 5 also shows that the structural evolution during the friction process mainly occurs at the interfacial rather than the intrinsic a-C region. In particular, it is well known that the friction behavior is highly sensitive to the complicated interface. In order to explore the underlying friction mechanism caused by different additives, the interfacial evolution including the binding states between the a-C, additives, and C<sub>8</sub>H<sub>16</sub> oil, the hybridized structure of interface, and the mobility of C<sub>8</sub>H<sub>16</sub> base oil and additives needs to be investigated. Before that, according to the atom distributions plotted in Fig. 5, the width of interfacial region is defined for each

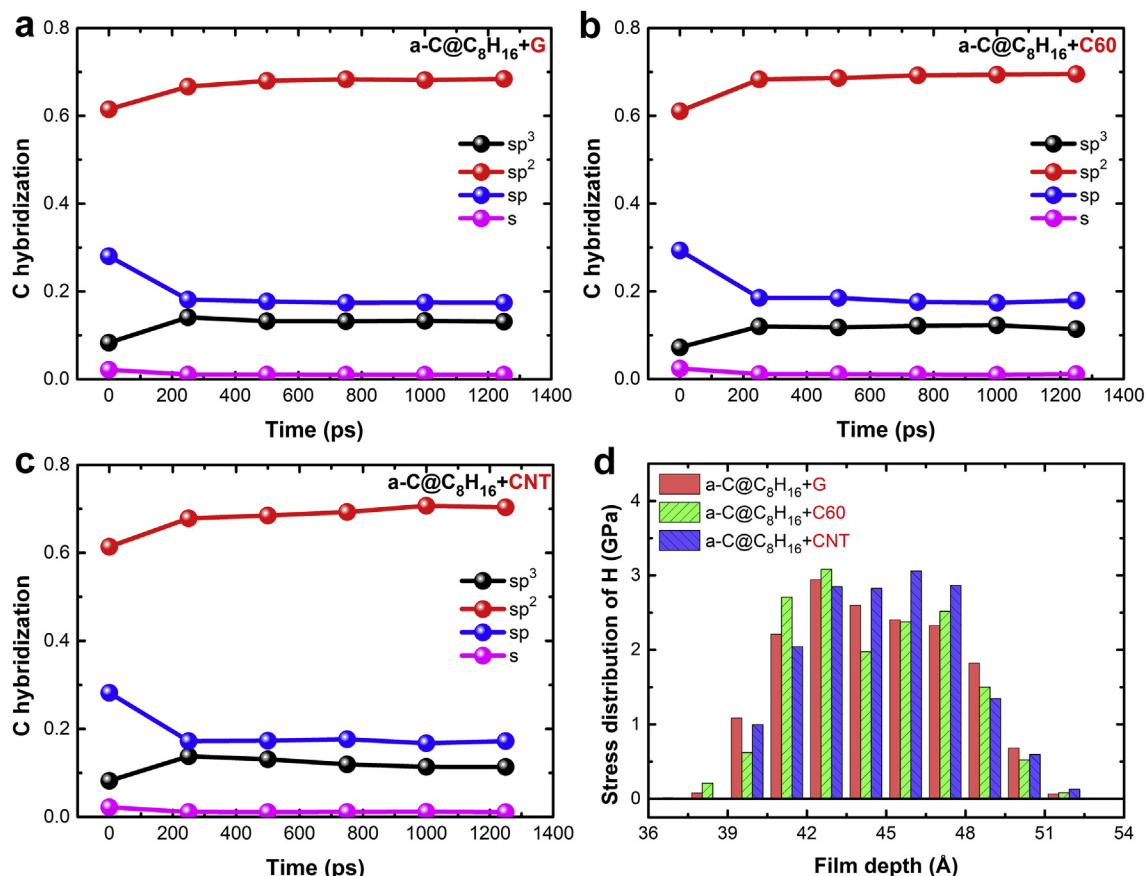


Fig. 8. Hybridized structure of interface with sliding time in (a) a-C@C<sub>8</sub>H<sub>16</sub>+G, (b) a-C@C<sub>8</sub>H<sub>16</sub>+C60, and (c) a-C@C<sub>8</sub>H<sub>16</sub>+CNT systems, which is only contributed by both the a-C and additives. (d) Stress distribution of H in C<sub>8</sub>H<sub>16</sub> base oil after the sliding process for each system. (A colour version of this figure can be viewed online.)

case, as shown in the area between the two dotted lines.

Before analyzing the evolution of interfacial structure, the binding state between the a-C, base oil, and additives needs to be discussed first. By the analysis of coordination number in Fig. 6, it reveals that the C<sub>8</sub>H<sub>16</sub> molecules interact with a-C mating materials or additives in the form of intermolecular interaction rather than chemical bonding due to the low activation energy caused by thermal or shearing effect [26]. There is also no degradation of C<sub>8</sub>H<sub>16</sub> molecules occurred during the sliding process, which coincides with previous study [3]. However, the chemical bonding between the additives and a-C is generated (Fig. 6) and especially followed by the different structural transformation of additive fragment during the sliding process, which plays a significant role in the friction process of a-C.

Using the specified interfacial region (Figs. 5), Fig. 7 illustrates the corresponding interfacial snapshots of a-C@C<sub>8</sub>H<sub>16</sub>+G, a-C@C<sub>8</sub>H<sub>16</sub>+C60, and a-C@C<sub>8</sub>H<sub>16</sub>+CNT systems with sliding time, in which the C<sub>8</sub>H<sub>16</sub> base oil is neglected for view. For a-C@C<sub>8</sub>H<sub>16</sub>+G system (Fig. 7a), the side carbon atoms from G fragment quickly interact with one a-C surface to form the covalent bonds. This leads to the G additive stably retained at the a-C surface during the friction process, but there is no obvious degradation of G due to low shearing effect (see inset in Fig. 7a and Fig. S2 of Supplementary Information) [36]. This is also suggested by the distribution of G in Fig. 5. In particular, due to the special 2D structure, the surface of graphene flake is parallel to the a-C surface, consistent with the sliding direction, which could shield the strong constraint of a-C dangling bonds to the base oil, improve the surface roughness, and thus bring little barrier to the mobility of C<sub>8</sub>H<sub>16</sub> base oil. This is consistent with previous experiment [37], in which the graphene fragments entered the water-boundary lubricated layer to reduce the direct contact zone between the specimen and the counter face.

Nevertheless, for a-C@C<sub>8</sub>H<sub>16</sub>+C60 system (Fig. 7b), C60 as additive can serve as a miniature bearing to lubricate the a-C surface by rolling or caterpillar motion [22], but the partial collapse of C60 structure occurs during the friction process due to the chemical bonding of C60 with both the a-C surfaces (see inset in Fig. 7b and Fig. S3 of Supplementary Information) [38]. Especially, when CNT as additive is introduced into the C<sub>8</sub>H<sub>16</sub> oil (Fig. 7c), it cannot exist stably at the friction interface. On the contrary, the strong chemical interaction of both the mating a-C surfaces with CNT side atoms results in the significant collapse of nanotube structure following the high roughness along the sliding direction (see inset in Fig. 7c and Fig. S4 of Supplementary Information). This has been confirmed by Matsumoto et al. in experiment [21]. Hence, during the sliding process, the C60 or CNT serves as a bridge to cross-link the two a-C surfaces, which is similar to Kuwahara's report [39]. This cross-linking will induce the high friction force and also potentially prevent the hydrodynamic effect of C<sub>8</sub>H<sub>16</sub> lubricant, although it may passivate the a-C surface to some extent. However, the graphene could anchor to the contact a-C surface and form a stable protective “tribofilm”, which significantly lubricates the contact surface and reduces the roughness, similar to previous reports [17,40,41].

Besides the interaction of a-C with additives, the analysis of interfacial hybridized structure is also essential to confirm its contribution to the friction reducing behavior [42–44]. Fig. 8a–8c display the evolution of hybridized structure of interface with sliding time for each case, in which only the contribution from both the a-C and additives is considered because of the absence of chemical bonding between the C<sub>8</sub>H<sub>16</sub> and a-C or additives (Fig. 6). Note that for each case, with the sliding time increased from 0 to 1250 ps, both the sp<sup>3</sup> and sp<sup>2</sup> fractions increase first and then become stable, which are followed by the reduction of sp fraction, suggesting the interfacial passivation during the sliding process.

This not only attributes to the interaction of sp-hybridized side atoms in additive fragment with the dangling C atoms of a-C surface (Fig. 7), but also to the self-passivation induced by the repulsive force of H atoms in C<sub>8</sub>H<sub>16</sub> base oil, as shown in Fig. 8d, which is also confirmed by Bai's study [34]. However, the hybridized structure of interface at the stable friction stage almost shows no dependence on the additive variety due to the low contact pressure, although the sp fraction in each case is slight higher than that in additive-free system due to the intrinsic side atoms with sp-hybridized state and tribo-induced degradation of additive structure.

Furthermore, the mean square displacements (MSD) for additive and C<sub>8</sub>H<sub>16</sub> base oil are estimated separately using the following equation [3,26], which is an essential tool to evaluate the effect of the mobility of fluid lubricant on the friction property.

$$MSD = r^2(t) = \frac{1}{N} \sum_{i=1}^N |r_i(t) - r_i(0)|^2 \quad (1)$$

where  $N$  is the number of  $i$  atoms in the system,  $r_i(t)$  and  $r_i(0)$  are the positions of the  $i$ th atom at time  $t$  and  $0$ , respectively. The MSD for additive in Fig. 9a further confirms the stable existence of G and C60 on the a-C surface via the chemical bonding, but a drastic increase of MSD is displayed for CNT due to the motion of dissociated CNT flakes caused by the strong bonding with two a-C surfaces. In particular, with the additive changed from G to C60 and CNT, the mobility of C<sub>8</sub>H<sub>16</sub> base oil decreases obviously, as illustrated in Fig. 9b, suggesting the deteriorated hydrodynamic lubrication of

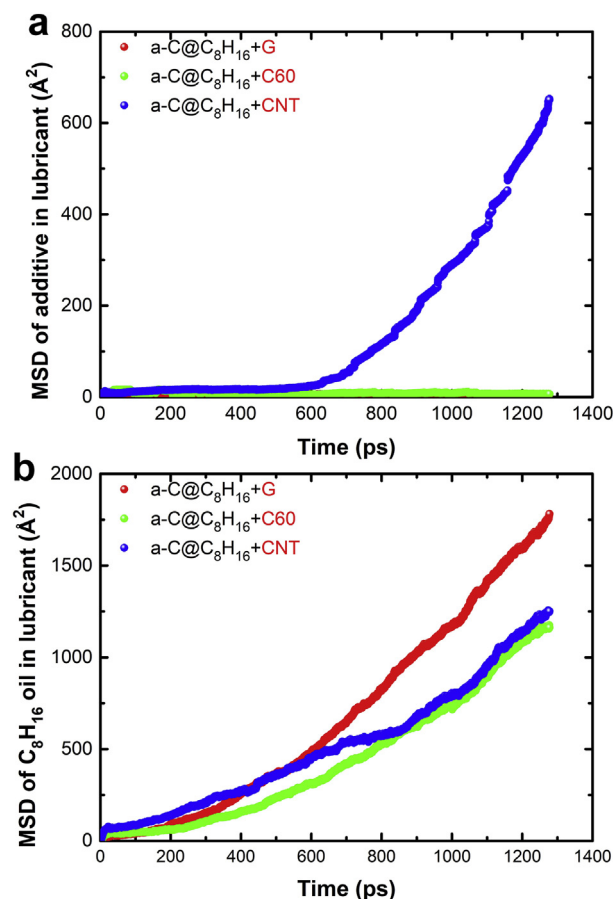


Fig. 9. MSD curves of the (a) additive and (b) C<sub>8</sub>H<sub>16</sub> base oil in fluid lubricant. (A colour version of this figure can be viewed online.)

$C_8H_{16}$  molecules. In the  $a-C@C_8H_{16}+G$  system, the G can effectively smooth the friction surface of a-C and also reduce the effect of a-C dangling bonds on the mobility of  $C_8H_{16}$  base oil, so the G and  $C_8H_{16}$  oil present a synergistic lubricating effect and thus lead to the superior lubricating performance as compared to that of the single component (G or  $C_8H_{16}$ ) [26]. However, in the system with C60 as additive, the dangling bonds from a-C and the cross-linking of C60 with both the mating a-C surfaces (Fig. 7b) will prohibit the  $C_8H_{16}$  molecules from moving along the  $x$ -sliding direction by the strong intermolecular interaction (Fig. 6), accounting for the increased friction coefficient, as shown in Fig. 3. When CNT is used as additive, the dangling bonds from both the a-C and dissociated CNT contribute to the reduced mobility of  $C_8H_{16}$  molecules, which is similar to the C60 case. But most importantly, the chemical interaction of CNT with both the a-C surfaces is enhanced significantly (Fig. 6) and the surface roughness is also increased due to the re-bonding of dissociated CNT flakes with a-C (Fig. 7c), resulting in the obvious increase of friction coefficient.

In addition, it should be mentioned that the content of additive in base oil plays a significant role on the lubricating performance [17]. The dependence of friction property and corresponding evolution of interfacial structure on G, C60, and CNT contents are presented in Fig. 10. Note that with increasing the G or C60 content from 0 wt% to 30.0 wt%, the friction coefficient decreases first and then increases for each case, agreeing well with previous experimental report [21], but the friction coefficient with CNT content increases monotonously. When the additive content is 30.0 wt%, the friction coefficients are 0.17 for G, 0.21 for C60, and 1.31 for CNT (Fig. 10a), respectively. In the  $a-C@C_8H_{16}+G$  system (Fig. 10b), with

increasing the G content, the G fragments interact with each other instead of the stable existence on the a-C surface. This not only leads to the G fragments piling up between the friction pairs, but also produces or aggravates the cross-linking interactions between the a-C surfaces, causing the increased friction coefficient (Fig. 10a). However, for C60 or CNT as oil-based additive, the behavior is similar to the case with low content, and the increase of friction coefficient results from the drastic enhancement of additive-linked bonding between the mating materials (Fig. 10c and d). Hence, this further indicates that the G is suggested to be the best candidate as oil-based additive than C60 and CNT to improve the friction behavior, and the base oil with low additive content, rather than high content, can more effectively improve the friction performance in synergism, which is in consistent with experimental study [45].

Fig. 10b and 10d also display that the additive with an excessive content, especially C60 and CNT, can affect the mobility of  $C_8H_{16}$  base oil or adsorb more oil molecules by strong intermolecular interaction. This induces the discontinuous distribution of base oil molecules and even brings the point-point contact or dry friction at the sliding interface, which also contributes to the friction performance [17,46]. Moreover, in the present work, the a-C without surface passivation is used to explore the additive-induced friction response. If the a-C surface is passivated by H, O, F et al. [42] or the multilayer graphene is used as additive, the friction property should be further improved due to the reduced intermolecular or chemical interaction between the a-C and fluid lubricant or the interlamination of graphene.

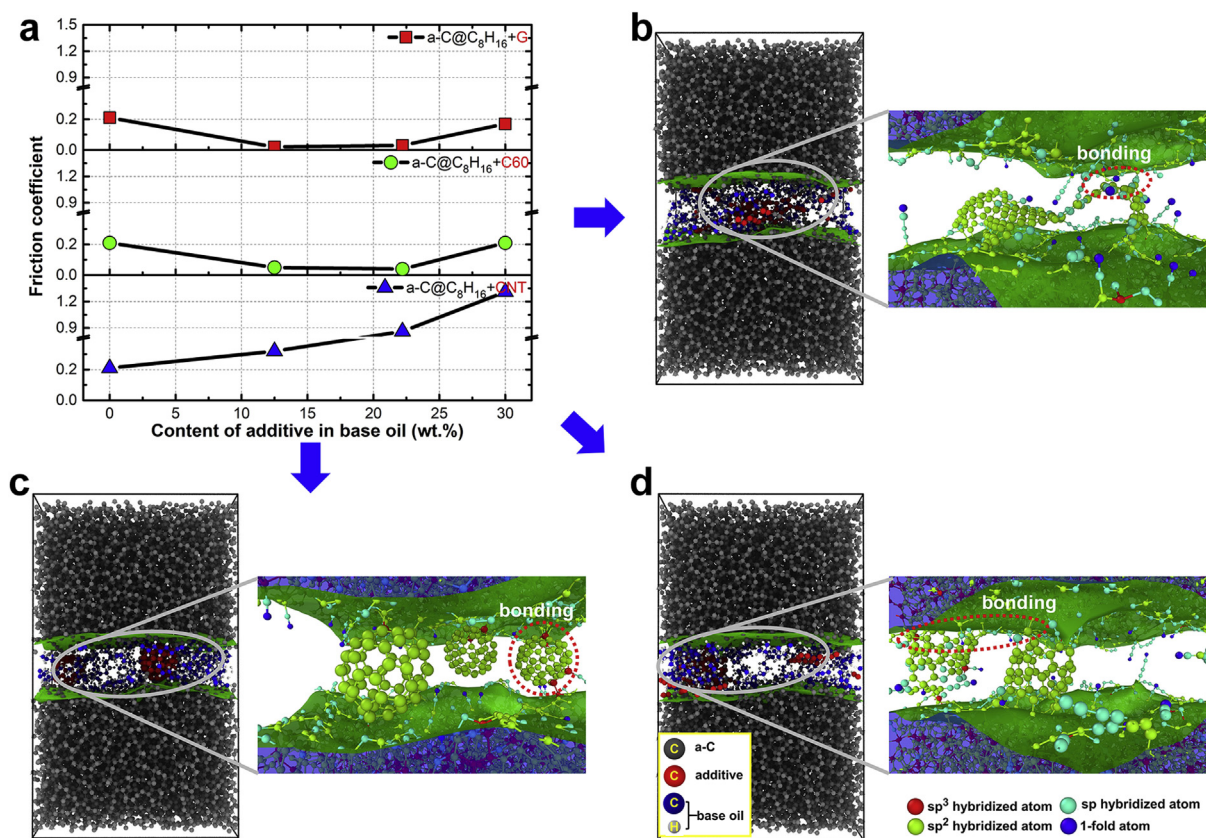


**Fig. 10.** Friction results of  $a-C@C_8H_{16}$  systems under different additive contents. (a) Evolution of friction coefficient with G, C60 or CNT content. Morphologies of (b)  $a-C@C_8H_{16}+G$ , (c)  $a-C@C_8H_{16}+C60$ , and (d)  $a-C@C_8H_{16}+CNT$  systems with additive content of 30.0 wt%, respectively, after the sliding process of 1000 ps, in which the insets are the local enlarged views for the hybridized interfacial structures. (A colour version of this figure can be viewed online.)

#### 4. Conclusions

We introduced carbon nanoparticles including G, C60, or CNT as oil-based additive to the a-C friction interface, and comparatively explored their effect on the friction behavior of a-C/fluid lubricant composite system using RMD simulation. By the systematical analysis of morphologies, the interaction between the a-C, base oil, and additives, the interfacial structure evolution, the stress distribution, the MSD of both the additive and base oil, and the friction property, results revealed that.

- ❖ Friction coefficient was strongly dependent on the additive variety in base oil. Compared with the additive-free case, adding G or C60 into the base oil resulted in the friction coefficient decreased by 90% or 76%, respectively, while the opposite increase of friction coefficient from 0.21 to 0.32 was observed for CNT as additive, demonstrating that the G could be used as an effective oil-based additive composited with a-C solid film for application.
- ❖ The fluid lubricant could effectively prevent the direct interaction between the contacting a-C films, in which the base oil component interacted with a-C and additives in the form of intermolecular interaction, but the chemical bonding occurred between the a-C and different additives.
- ❖ In a-C/C<sub>8</sub>H<sub>16</sub>+G system, the G bonded with a-C surface to form a protective film, which not only improved the surface roughness, but also shielded the strong constraint of a-C dangling bonds to the base oil, causing the significant reduction of friction coefficient in synergism with the excellent mobility of base oil, as compared to that of the single component. However, although C60 served as a miniature bearing to lubricate the surface by caterpillar motion, the cross-linking of C60 with both the a-C surfaces restricted the sliding of a-C and the hydrodynamic effect of base oil. Especially for CNT, the strong chemical bonding between the a-C surfaces and CNT brought the drastic collapse of nanotube structure and high roughness, accounting for the increase of friction coefficient.
- ❖ Furthermore, the lubricating efficiency was also related with the additive content in base oil, and the excessive content for each additive was accompanied by the increased friction coefficient, mainly attributing to the piling up between the additives and the aggravated chemical interactions of additives with both the a-C surfaces.
- ❖ The present results disclose the fundamental friction mechanism caused by carbon nano-additives and provide guidance to develop the new fluid lubricant and the advanced a-C/fluid lubricating system through tailoring the composition and content of nano-additives for potential applications.

#### Acknowledgments

This research was supported by the Korea Research Fellowship Program funded by the Ministry of Science and ICT through the National Research Foundation of Korea (2017H1D3A1A01055070), the Nano Materials Research Program through the Ministry of Science and IT Technology (NRF-2016M3A7B4025402), the National Natural Science Foundation of China (51772307), and Zhejiang Key Research and Development Program (2017C01001).

#### Appendix A. Supplementary data

Supplementary data to this article can be found online at <https://doi.org/10.1016/j.carbon.2019.05.050>.

#### References

- [1] S. Zhang, T. Ma, A. Erdemir, Q. Li, Tribology of two-dimensional materials: from mechanisms to modulating strategies, *Mater. Today* (2018), <https://doi.org/10.1016/j.mattod.2018.12.002>.
- [2] K. Holmberg, A. Erdemir, Influence of tribology on global energy consumption, costs and emissions, *Friction* 5 (2017) 263–284.
- [3] X. Li, A. Wang, K.R. Lee, Mechanism of contact pressure-induced friction at the amorphous carbon/alpha olefin interface, *npj Comput Mater* 4 (2018) 53.
- [4] L. Zhang, J. Pu, L. Wang, Q. Xue, Frictional dependence of graphene and carbon Nanotube in diamond-like carbon/ionic liquids hybrid films in vacuum, *Carbon* 80 (2014) 734–745.
- [5] X. Liu, L. Wang, Q. Xue, DLC-based solid–liquid synergetic lubricating coatings for improving tribological behavior of boundary lubricated surfaces under high vacuum condition, *Wear* 271 (2011) 889–898.
- [6] L. Wang, L. Cui, Z. Lu, H. Zhou, Understanding the unusual friction behavior of hydrogen-free diamond-like carbon films in oxygen atmosphere by first-principles calculations, *Carbon* 100 (2016) 556–563.
- [7] H.A. Tasdemir, M. Wakayama, T. Tokoroyama, H. Kousaka, N. Umehara, Y. Mabuchi, T. Higuchi, Ultra-low friction of tetrahedral amorphous diamond-like carbon (ta-C DLC) under boundary lubrication in poly alpha-olefin (PAO) with additives, *Tribol. Int.* 65 (2013) 286–294.
- [8] Z. Jia, Y. Xia, J. Li, X. Pang, X. Shao, Friction and wear behavior of diamond-like carbon coating on plasma nitrided mild steel under boundary lubrication, *Tribol. Int.* 43 (2010) 474–482.
- [9] J.M. Martin, M.I.D.B. Bouchet, C. Matta, Q. Zhang, W.A. Goddard III, S. Okuda, T. Sagawa, Gas-phase lubrication of ta-C by glycerol and hydrogen peroxide. experimental and computer modeling, *J. Phys. Chem. C* 114 (2010) 5003–5011.
- [10] H. Okubo, C. Tadokoro, S. Sasaki, Tribological properties of tetrahedral amorphous carbon (ta-C) film under boundary lubrication in the presence of organic friction modifiers and zinc dialkyldithiophosphate (ZDDP), *Wear* 332–333 (2015) 1293–1302.
- [11] J. Zhao, J. Mao, Y. Li, Y. He, J. Luo, Friction-induced nano-structural evolution of graphene as a lubrication additive, *Appl. Surf. Sci.* 434 (2018) 21–27.
- [12] L. Austin, T. Liskiewicz, I. Kolev, H. Zhao, A. Neville, The influence of anti-wear additive ZDDP on doped and undoped diamond-like carbon coatings, *Surf. Interface Anal.* 47 (2015) 755–763.
- [13] C.S. Chen, X.H. Chen, L.S. Xu, Z. Yang, W.H. Li, Modification of multi-walled carbon nanotubes with fatty acid and their tribological properties as lubricant additive, *Carbon* 43 (2005) 1660–1666.
- [14] B. Liu, H. Li, Alkylated fullerene as lubricant additive in paraffin oil for steel/steel contacts, *Fullerenes, Nanotub. Carbon Nanostruct.* 24 (2016) 712–719.
- [15] V. Eswarajah, V. Sankaranarayanan, S. Ramaprabhu, Graphene-based engine oil nanofluids for tribological applications, *ACS Appl. Mater. Interfaces* 3 (2011) 4221–4227.
- [16] V. Zin, S. Barison, F. Agresti, L. Colla, C. Pagura, M. Fabrizio, Improved tribological and thermal properties of lubricants by graphene based nano-additives, *RSC Adv.* 6 (2016) 59477–59486.
- [17] Y. Meng, F. Su, Y. Chen, Au/graphene oxide nanocomposite synthesized in supercritical CO<sub>2</sub> fluid as energy efficient lubricant additive, *ACS Appl. Mater. Interfaces* 9 (2017) 39549–39559.
- [18] T. Luo, X. Chen, P. Li, P. Wang, C. Li, B. Cao, J. Luo, S. Yang, Laser irradiation-induced laminated graphene/MoS<sub>2</sub> composites with synergistically improved tribological properties, *Nanotechnology* 29 (2018) 265704.
- [19] J. Mao, J. Zhao, W. Wang, Y. He, J. Luo, Influence of the micromorphology of reduced graphene oxide sheets on lubrication properties as a lubrication additive, *Tribol. Int.* 119 (2018) 614–621.
- [20] Y. Yao, X. Wang, J. Guo, X. Yang, B. Xu, Tribological property of onion-like fullerenes as lubricant additive, *Mater. Lett.* 62 (2008) 2524–2527.
- [21] N. Matsumoto, K.K. Mistry, J.H. Kim, O.L. Eryilmaz, A. Erdemir, H. Kinoshita, N. Ohmae, Friction reducing properties of onion-like carbon based lubricant under high contact pressure, *Tribotest* 6 (2012) 116–120.
- [22] P. Zhang, J. Lu, Q. Xue, W. Liu, Microfrictional behavior of C60 particles in different C60 LB films studied by AFM/FFM, *Langmuir* 17 (2001) 2143–2145.
- [23] K. Gong, X. Wu, G. Zhao, X. Wang, Tribological properties of polymeric aryl phosphates grafted onto multi-walled carbon nanotubes as high-performance lubricant additive, *Tribol. Int.* 116 (2017) 172–179.
- [24] Y. Meng, F. Su, Y. Chen, Nickel/multi-walled carbon nanotube nanocomposite synthesized in supercritical fluid as efficient lubricant additive for mineral oil, *Tribol. Lett.* 66 (2018) 134.
- [25] N. Salah, MSh Abdel-wahab, A. Alshahrie, N.D. Alharbi, Z.H. Khan, Carbon nanotubes of oil fly ash as lubricant additives for different base oils and their tribology performance, *RSC Adv.* 7 (2017) 40295–40302.
- [26] X. Li, A. Wang, K.R. Lee, Tribo-induced structural transformation and lubricant dissociation at amorphous carbon-alpha olefin interface, *Adv Theory Simul* 2 (2019) 1800157.
- [27] S. Plimpton, Fast parallel algorithms for short-range molecular dynamics, *J. Comp. Physiol.* 117 (1995) 1–19.
- [28] X. Li, P. Ke, H. Zheng, A. Wang, Structure properties and growth evolution of diamond-like carbon films with different incident energies: a molecular dynamics study, *Appl. Surf. Sci.* 273 (2013) 670–675.
- [29] H.J.C. Berendsen, J.P.M. Postma, W.F. van Gunsteren, A. DiNola, J.R. Haak, Molecular dynamics with coupling to an external bath, *J. Chem. Phys.* 81

- (1984) 3684–3690.
- [30] F. Tavazza, T.P. Senftle, C. Zou, C.A. Becker, A.C.T. Van Duin, Molecular dynamics investigation of the effects of tip-substrate interactions during nano-indentation, *J. Phys. Chem. C* 119 (2015) 13580–13589.
- [31] X. Li, A. Wang, K.R. Lee, Insights on low-friction mechanism of amorphous carbon films from reactive molecular dynamics study, *Tribol. Int.* 131 (2019) 567–578.
- [32] G. Zilibotti, S. Corni, M.C. Righi, Load-induced confinement activates diamond lubrication by water, *Phys. Rev. Lett.* 111 (2013) 146101.
- [33] T.B. Ma, L.F. Wang, Y.Z. Hu, X. Li, H. Wang, A shear localization mechanism for lubricity of amorphous carbon materials, *Sci. Rep.* 4 (2014) 3662.
- [34] S. Bai, H. Murabayashi, Y. Kobayashi, Y. Higuchi, N. Ozawa, K. Adachi, J.M. Martin, M. Kubo, Tight-binding quantum chemical molecular dynamics simulations of the low friction mechanism of fluorine-terminated diamond-like carbon films, *RSC Adv.* 4 (2014) 33739–33748.
- [35] Y. Mo, K.T. Turner, I. Szlufarska, Friction laws at the nanoscale, *Nature* 457 (2009) 1116–1119.
- [36] L. Zhang, J. Pu, L. Wang, Q. Xue, Synergistic effect of hybrid carbon nanotube-graphene oxide as nanoadditive enhancing the frictional properties of ionic liquids in high vacuum, *ACS Appl. Mater. Interfaces* 7 (2015) 8592–8600.
- [37] X. Ye, L. Ma, Z. Yang, J. Wang, H. Wang, S. Yang, Covalent functionalization of fluorinated graphene and subsequent application as water-based lubricant additive, *ACS Appl. Mater. Interfaces* 8 (2016) 7483–7488.
- [38] R. Greenberg, G. Halperin, I. Etsion, R. Tenne, The effect of WS<sub>2</sub> nanoparticles on friction reduction in various lubrication regimes, *Tribol. Lett.* 17 (2004) 179–186.
- [39] T. Kuwahara, P.A. Romero, S. Makowski, V. Weihnacht, G. Moras, M. Moseler, Mechano-chemical decomposition of organic friction modifiers with multiple reactive centers induces superlubricity of ta-C, *Nat. Commun.* 10 (2019) 151.
- [40] S. Liang, Z. Shen, M. Yi, L. Liu, X. Zhang, S. Ma, In-situ exfoliated graphene for high-performance water-based lubricants, *Carbon* 96 (2016) 1181–1190.
- [41] X. Liu, J. Pu, L. Wang, Q. Xue, Novel DLC/ionic liquid/graphene nanocomposite coatings towards high-vacuum related space applications, *J. Mater. Chem.* 1 (2013) 3797–3809.
- [42] Y.N. Chen, T.B. Ma, Z. Chen, Y.Z. Hu, H. Wang, Combined effects of structural transformation and hydrogen passivation on the friction behaviors of hydrogenated amorphous carbon films, *J. Phys. Chem. C* 119 (2015) 16148–16155.
- [43] L. Cui, Z. Lu, L. Wang, Probing the low-friction mechanism of diamond-like carbon by varying of sliding velocity and vacuum pressure, *Carbon* 66 (2014) 259–266.
- [44] X. Chen, C. Zhang, T. Kato, X. Yang, S. Wu, R. Wang, M. Nosaka, J. Luo, Evolution of tribo-induced interfacial nanostructures governing superlubricity in a-C:H and a-C:H:Si films, *Nat. Commun.* 8 (2017) 1675.
- [45] K. Fan, X. Chen, X. Wang, X. Liu, Y. Liu, W. Lai, X. Liu, Toward excellent tribological performance as oil-based lubricant additive: particular tribological behavior of fluorinated graphene, *ACS Appl. Mater. Interfaces* 10 (2018) 28828–28838.
- [46] W. Zhang, M. Zhou, H. Zhu, Y. Tian, K. Wang, J. Wei, F. Ji, X. Li, Z. Li, P. Zhang, D. Wu, Tribological properties of oleic acid-modified graphene as lubricant oil additives, *J. Phys. D Appl. Phys.* 44 (2011) 205303.